Towards transparent and durable copper-containing antimicrobial surfaces

Check for updates

Christina Graham[1], Alessia Mezzadrelli[1], Wageesha Senaratne[2] ✉, Santona Pal[2], Dean Thelen[2], Lisa Hepburn[2], Prantik Mazumder [2] & Valerio Pruneri [1,3] ✉

Metallic copper is a potent antimicrobial agent with high efficacy against a range of microorganisms. Whilst it is commonplace for objects such as door handles and hospital bedrails to be made of or to be coated with copper, other high-touch surfaces such as those of screens and monitors would lose their optical transparency. Herein, we report the design of a transparent antimicrobial nanostructured copper surface obtained by dewetting ultrathin metal copper films on glass. Antimicrobial effectiveness of >99.9 % was obtained within 2 h against Staphylococcus aureus following the US Environmental Protection Agency Test method. Moreover, the proposed surfaces show an average transmittance between 70–80% with little color in the visible range. Additionally, they maintain optical and antimicrobial properties after abrasion and chemical exposure tests designed to replicate physical wear and repeated exposure to biocidal cleaning materials. With the demonstrated surfaces' antimicrobial, colorless, and durability properties, they have potential in applications such as touch-enabled public or personal displays once higher transparency is achieved.

In recent years, the potential of surfaces to harbor harmful microorganisms has attracted great attention. Together with increased awareness, there is now a growing demand for effective disinfection practices of personal and multi-user touch activated displays, in which traditional methods such as sprayable alcohol are impractical. More specifically, coatings containing antimicrobial (AM) constituents are a promising solution for glass, when they are transparent, durable during its use case and resistant to general use wear-and-tear[1–3].

Several reports have promoted the use of nanostructured or ultrathin metals and their oxides in transparent applications including directly into the glass itself or as part of a surface coating. Popular approaches of surface coatings include the use of photocatalytic metal oxides such as titanium dioxide (TiO_2) or zinc oxide (ZnO)[1,2]. These materials interact with moisture and light to produce bactericidal reactive oxygen ion species which are harmful to the microbes present on the surface. Whilst effective, these coatings are light activated and would not be suitable for indoor environments. Subsequent coating studies have explored the combination of pure metallic species with photocatalytic oxides to afford dual-functionality coatings with AM function irrespective of light availaibility[3,4]. In addition, recently, ion-exchanged glass has been touted as a promising approach. In this, sodium ions near the glass surface are exchanged for silver ions in an ion exchange process. This leads to the formation of an AM Ag-ion

containing diffusive layer in the surface of the glass[5]. These have superb optical performance but rapid bacterial burden reduction (as tested pursuant to US EPA protocol) is a challenge.

The use of Cu in various supporting media has been highly reported in AM coatings for bedrails and intravenous stand poles[6,7] in hospital settings as well as for AM glass ceramics[8]. However, for application on transparent high-touch surfaces such as tablets and mobile devices, a high level of transparency of the overlying antibacterial coating is essential to preserve the functionality of the device. To achieve transparency, Cu ions have previously been embedded into or deposited on top of a polymer matrix[9–11] or in a nanocomposite with SiO_2[12–15]. The AM activity of copper-containing surfaces is dependent on their ability to release free Cu ions (i.e Cu^+ and Cu^{2+}) by aqueous corrosion processes[16,17]. The dominant process(es) taking place are determined by the starting oxidation state of the copper, the prevailing environmental (e.g., relative humidity, temperature) and chemical conditions (e.g., air constituents, sweat contaminants). Once released, the Cu^+/Cu^{2+} exert cytotoxic effects by participating in cyclic redox reactions at the cell surface[18]. For example, charged ions may accumulate on the negatively charged domains of the bacterial membrane, altering its permeability and causing leakage of intracellular components[19]. Ion channels within the membrane also permit the transport of nanoparticles (NPs) into bacterial cells where they release ions, which subsequently generate intracellular

[1]ICFO-Institut de Ciències Fotòniques, The Barcelona Institute of Science and Technology, 08860 Castelldefels, Barcelona, Spain. [2]Corning Research and Development Corporation, Sullivan Park, Corning, New York, NY 14831, USA. [3]ICREA-Institució Catalana de Recerca i Estudis Avançats, 08010 Barcelona, Spain. ✉e-mail: senaratnw@corning.com; valerio.pruneri@icfo.eu

reactive oxygen species (ROS) including hydrogen peroxide (H_2O_2), superoxide ($O_2^{\cdot-}$), hydroxyl radical ($^{\cdot}OH$), and singlet oxygen[20]. These species induce oxidative stresses to intracellular components, denature proteins, alter the structure of DNA and de-regulate cellular metabolism[21–24].

Whilst Cu has been demonstrated as a potent AM agent[9,13,25–30], a Cu containing transparent AM coating is yet to be fully realized due to the opacity of metallic copper and oxide coatings. Furthermore, for applications such as touch-enabled public or personal displays, lack of electrical insulation destroys the touch functionality. In this regard, Behzadinasab et al. developed two transparent, sprayable polydopamine (PDA) & copper-based surface coatings for glass[10]. Using a thin layer of copper deposited on a PDA layer, they achieved a reduction of >99.99% of *P. aeruginosa* and 99.18% of MRSA within 10 min compared to a glass control, as well as 99.98% reduction of SARS-CoV-2 virus in 1 h. Using a sparse layer of Cu_2O bound to the PDA, they obtained a reduction of 99.94% of *P. aeruginosa* and 96.82% of MRSA within 10 min, as well as 99.88% of SARS-CoV-2 virus in 1 h compared to a glass control. The same group also tested transparent AM coatings of silver oxide particles in a silicate matrix on glass[31]. The coatings demonstrated at least a 99.8% decrease in SARS-CoV-2, MRSA, *S. aureus*, and *P. aeruginosa* in 1 h, and were transparent and allowed retain touch screen function[31].

In this work, we present a design of a transparent, non-conductive, AM nanostructured Cu surface (TANCS) on glass substrates. Our design satisfies several criteria; (1) the Cu release rate is be controlled by a supporting medium such that coating remains permanently AM and still transparent; (2) the coating imparts the desired AM function without altering the original performance of the substrate; (3) the Cu film or nanoparticles when deposited on substrate do not impact significantly the transparency and color of the original substrate; (4) the surfaces with the nanostructured coating are durable and retain their AM property, after repeated and extended use; for example, they should be resistant to oxidation (the transformation of Cu into CuO_x leads to a lessening of AM effect) and mechanical abrasion.

The TANCS demonstrated a high average transparency, i.e., average transmission including substrate between 70% and 80% in the range of 380–750 nm, flatness of transmission in the visible range, thereby, producing no distracting color effect, killing over 99.9% of *Staphylococcus aureus* within 2 h and maintaining the AM activity after rigorous wipe testing in accordance to the EPA 'Test Method for Efficacy of Cu Alloy Surfaces as a Sanitizer'[32]. Our design and method entail thermal dewetting of ultrathin metal films (UTMFs) to form dewetted Cu nanoparticles (Cu DNPs) with optimized size for providing the AM effect, transparency, color neutrality and electrical insulation. The design, shown schematically in Fig. 1, also includes additional functional layers of SiO_2 and fluorosilanes, which are deposited conformally on top of the dewetted Cu DNPs. Together, these additional layers provide an easy means of tuning Cu exposed to the environment and microbes. In addition, by anchoring the particles to the substrate, they enhance the coating's durability and protect against environmental oxidation, external chemical agents, and mechanical forces without sacrificing its overall transparency.

In this paper, TANCS morphology, transmittance, AM efficacy, mechanical durability, and trade-offs of these properties were investigated. Metal dewetting for nanostructuring the surface of glass substrates has already been used[33–37]. However, to our knowledge, it is the first time it has been used for AM properties. Such process has the advantage of being simple and scalable as it does not rely on time-consuming and sophisticated lithography techniques (e.g., electron beam and nanoimprint). Finally, being electrically insulating, TANCS would be appropriate for application in capacitive touch-activated devices.

Methods
Fabrication of TANCS
Ion-exchanged glass substrates from Corning Incorporated (Gorilla® Glass®) with a size of 2×2 in.^{2} and 0.3 mm thickness were sonicated in conventional organic solvents for 10 min and dried with an N_2 gun. For comparative experiments, where the dewetting process was performed at temperature greater than the IOX-exchanged glass strain point, fused silica substrates were used (Results and discussion). A magnetron sputtering system (ATC Orion 8, AJA International, Inc.) was used for the metal depositions. A pre-deposition cleaning of the substrates was performed by exposing the substrates to an Ar plasma (bias power 40 W, pressure 8 mT, Ar flow 20 standard cubic centimeters per minute (scc/min)) for 5 min. An ultrathin titanium (Ti) adhesion layer with a thickness of 2 nm onto the flat glass substrates was deposited from a target of 99.7% purity with a Direct Current (DC) power of 100 W and a working pressure of 2 mTorr in an argon atmosphere (20 scc/min). This was followed by a deposition of an ultrathin Cu film with a thickness of 3.5 nm as shown in Fig. 1. The Cu film thickness was controlled by the sputtering time. The depositions were performed at a base pressure between 10^{-7} and 10^{-8} Torr, room temperature, 100 W of DC power, and 20 scc/min of pure argon (Ar). The working pressure was 1.5×10^{-3} Torr, the deposition rate was estimated to be 0.0454 nm/s for Ti and 0.142 nm/s for Cu, and the target−substrate distance was 35 cm with a rotation speed of 60 rpm. To obtain nanoparticles, the samples were subjected to a rapid thermal annealing (RTA) process as shown in Fig. 2. The RTA was carried out in the Tsunami TM RTP-600S system at the temperature of 390 °C, below the glass strain point temperature of the substrate (580 °C), for 600 s. High-purity N_2 gas (1 atm pressure) was used to reduce the oxidation of the metal film. After RTA, 10 to 50 nm of SiO_2 were deposited conformally onto the Cu nanoparticles by using E-beam evaporation system (Lesker LAB 18 Thin Film Deposition System), as shown in Fig. 1. The deposition was performed at a base pressure between 10^{-7} and 10^{-8} Torr, room temperature. The SiO_2 E-beam evaporation rate was set to 1 A/s as measured by a quartz microbalance. Thickness tested ranged between 0 and 50 nm to provide partial coverage the nanoparticles whilst allowing optimization of the durability and AM property of the coating. As a final step, the nanostructured surface may be coated with a low surface energy coating, such as a fluorosilane. Both continuous and patterned fluorosilane coating methods were evaluated to obtain the best performance. Prior to the fluorosilane application, the coated substrates were cleaned with an oxygen plasma of strength between 50–300 W for a time of 2–5 min. The fluorosilane used in this work was Optool UD509 obtained from Daikin Chemicals and it was diluted to 0.005–0.024 % by weight in a fluorinated solvent (Novec HFE7200) obtained from 3 M Company. The fluorosilane was deposited onto the substrate by spray-coating using an airbrush. The airbrush was held 2 in. away from the AM coating and sprayed for 20 s to enable even coverage. In cases where patterned coverage was desired, a mask was used. The pressure of the airbrush was varied between 6 and 35 psi. Finally, the fluorosilane was cured at 150 °C, <10 min or in a desiccator at room temperature (RT) for 2 days. The coating was then rinsed or sonicated in fluorinated solvent (NovecTM HFE7200 from 3 M Company) for a time of 3–5 min to remove excess material. In this work, AM efficacy against *S.Aureus* was performed on 3 sets of TANCSs, with varying SiO_2 thickness, fluorosilane concentration and oxidation conditions, according to Table 1. A schematic of the fabrication process is provided in Supplementary Fig. 1.

Antimicrobial (AM) efficacy testing of TANCS
Bactericidal efficacy testing on the TANCSs, stainless steel (SS), uncoated glass and Cu control samples were performed as described in the EPA test for efficacy of Cu alloy surfaces as a sanitizer[32]. Each coupon was tested in duplicate. Prior to AM testing, all coupons were cleaned by immersion in a 75% ethanol solution followed by rinsing with deionized (DI) water. The coupons were then sterilized by exposure to ultraviolet (UV) light at 254 nm, for a duration of 15 min. For the preparation of the inoculum, a 20 μL aliquot of thawed bacterial *Staphylococcus aureus AT 6538 (S.Aureus)* culture was added to 10 mL Tryptic Soy Broth. The bacterial suspension was incubated at 36 °C for 48 h. The culture was subsequently centrifuged and allowed to settle as a pellet. The supernatant was removed and pellet was resuspended in 6 mL of phosphate buffer saline (PBS). The upper two thirds of suspension were aspirated and the optical density at 600 nm (OD600) was

measured to obtain the bacterial density estimation. The cell culture was diluted with PBS to achieve a bacterial inoculum concentration near the target value of 1.0×10^6 colony-forming units (CFU) mL^{-1}. Organic soil load containing 250 μL fetal bovine serum (FBS) and 50 μL TritonX were added to 4700 μL of the inoculum. Here, FBS is used as a universal growth supplement for in vitro culture and TritonX to aid in spreading of the inoculum on the substrates. Each coupon was inoculated with 20 μL of inoculum, that was spread evenly over a central 1×1 in.^{2} test area of the coupon using bent sterile pipette tips. The 20 μL on the coupon typically dry within 5–15 min in ambient conditions. Once dry, the coupons were incubated in a controlled environment set at 42% relative humidity (RH) and 23 °C for a period of 2 h. Following the 2 h exposure period, the coupons were neutralized in Letheen broth (Gen Lab). Ten-fold serial dilutions of the neutralized solutions were plated using standard spread plate technique on Tryptic Soy Agar plates and incubated for 48 h at 36 °C to yield countable numbers of survivors (~20–200 colonies per plate). This range was selected because below 20 CFUs it gives poor counting statistics and above 200 CFUs the bacteria grow too close to each others.

Calculations of log and percentage of reductions

The calculation of the value of the AM activity is based on the difference between the mean number of the log$_{10}$ of bacteria surviving on the TANCS
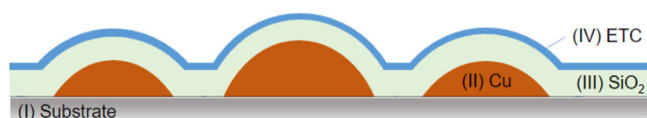

Fig. 1 | Schematic illustration of the TANCS. They comprise: (I) 0.3 mm thick CORNING® GORILLA® GLASS substrate, (II) dewetted Cu nanoparticles (NPs) from a UTMF of 3.5 nm Cu, (III) SiO$_2$ embedding layer and (IV) Easy-To-Clean (ETC) Fluorosilane coating. Dimensions are not in scale. The difference in shape (e.g., contact angle) of the particles reflects the real images, an example being that shown in Fig. 2.

test and the mean number of the log$_{10}$ of bacteria surviving on the glass cover slip control samples according to the EPA protocol provided in the Supplementary Note 2[32]. The experiments were performed in duplicate. For the coatings to be approved as a "self-sanitizing", the AM test must demonstrate at least a 3-Log Reduction (3-LR) within the specified contact time. This corresponds to a 99.9% reduction in CFUs.

Stipulated wear testing

TANCSs were subjected to a modified cleaning regimen suitable for electronic glass display covers based on EPA test method for efficacy of copper alloy surfaces as a sanitizer[32]. The cleaning regimen was designed to test the durability of the TANCS against abrasion from wiping with a cleaning cloth, frequent contact with a pants pocket or purse during removal and insertion, touching with a human finger, and/or chemical interaction with the environment or cleaning solutions. The abrasion procedures simulate regular touch and a worst-case scenario of 2× cleaning every day for up to 2 years. Simulated wear was performed using an Elcometer 5750 Taber® Linear Abrader. For wet abrasion, the cleaning solution was prepared with either isopropanol (IPA) and deionized (DI) water (70:30) or Lysol®. A cover glass wipe was saturated with cleaning solution and attached to the abrader head using double-sided adhesive tape. No additional weights were added to the spline-shaft of the linear abrader (base load of 350 g) in order to keep the pressure similar to that applied in by repeated touch or cloth wipes. One complete wear cycle consisted in 2 passes of the wet (or dry) cover glass wipe against the test surface. This process was repeated for 700–1200 cycles (1400–2400 passes of the wet scouring pad) to simulate wear and cleaning for up to 2 years. After completion of the wear cycles, the 'worn' surfaces were tested for bacterial efficacy against *S.Aureus* using the EPA testing procedure detailed in "Antimicrobial (AM) efficacy testing of TANCS".

Inductively coupled mass spectroscopy (ICP-MS) mock testing to characterize amount of leached copper from TANCS

The number of Cu ions from coating that equilibrate with those in the liquid inoculum in the AM test was estimated using a mock test that mimics the
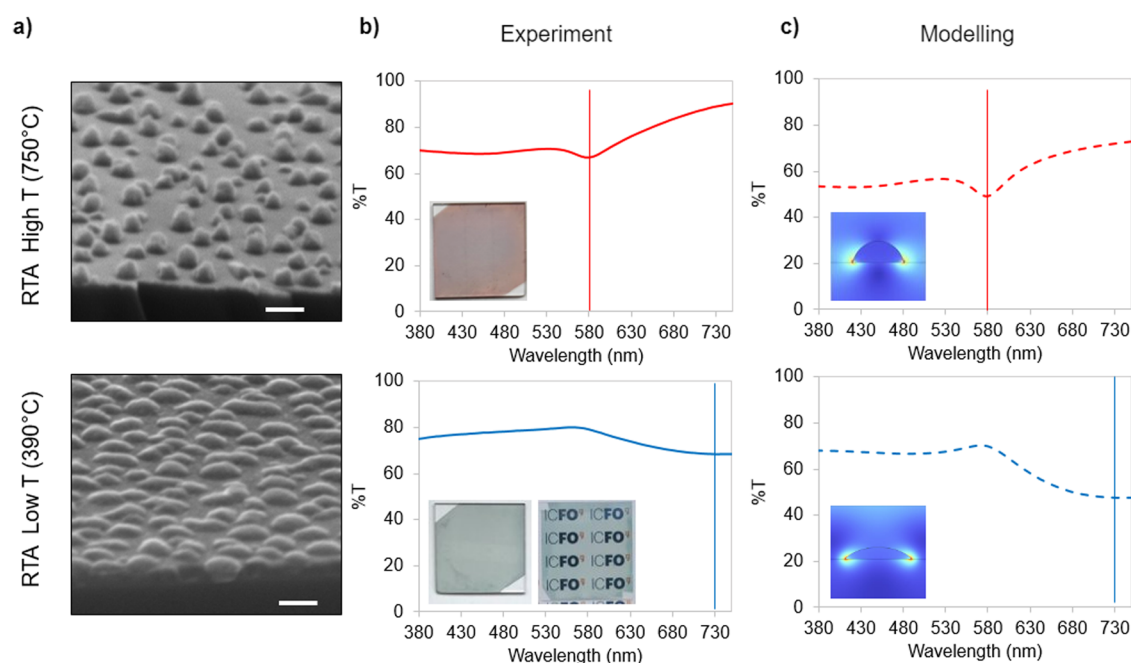

Fig. 2 | Morphological properties and optical response of CuDNPs. SEM images (**a**) clearly illustrate the influence of the annealing temperature on the particle shape and size. High temperature produces separate, rounded particles with a contact angle ≈90°, whilst low temperature produces, flatter particles, with a contact angle < 90° and that are sometimes in contact. Scale bar = 100 nm. Optical spectra obtained from experiment (**b**) and modeling (**c**). Modeling qualitatively reproduces the experiments, in particular the red shift and broadening of the plasmonic resonance due to a reduction of particle's contact angle. Insets of (**b**) show the color of the coatings against white background and also against a colored text background to show transparency and color neutrality of the TANCS. The size of the samples is 2 x 2 in.^{2}. The insets of (**c**) show the particle shape used for the modeling as determined from the SEM images in a.

Table 1 | TANCS coatings (A and B type) together with control (ctrl) samples

Set	Plasma (Power and Time)	SiO$_2$ (nm)	Fluorosilane concentration (%)
Ctrl: Uncoated glass	-	-	-
Ctrl: Stainless steel	-	-	-
Ctrl: Cu pure	-	-	-
A	50 W 2 min	20–25–30–35–50	0
		20–25–30–35–50	0.012
		35–50	0.024
B	300 W 5 min	0–10–15	0
		15–25	0.005
		0–10–15–25	0.012
		10–15	0.024

AM test—the mock test keeps all conditions the same as the AM test except it has no bacteria in the inoculum. The control and test coupons are treated with the same cleaning and sterilization process as for the EPA AM test (see in the Supplementary Note 2). 20 µL aliquot of inoculum (without bacteria) was added to the central 1 in.^{2} area of the TANCS. The leaching was performed in controlled environment set at 42% RH and 23 °C for a period of 2 h. The leachate was collected from the coating by using 2×150 µL of PBS in the exposed 1 in.^{2} region, rinsing and removing the rinse solution into a tube. The amount of Cu in the leached solution was determined using ICP/MS detection. Positive and negative controls were run with pure Cu and stainless steel coupons, respectively. The optical response of the coating after mock testing in the region 350–750 nm was also obtained.

Morphological, optical, mechanical, and antimicrobial characterizations of the coatings

The optical transmission spectra of the coatings in the wavelength range 380–750 nm was acquired using a spectrometer (Perkin Elmer LAMBDA 950). All of the reported transmission spectra represent the substrate and coating i.e., bare (uncoated) glass + Ti adhesion layer + dewetted Cu + SiO$_2$ + fluorosilane. Haze measurements were obtained using a BYK Haze-Guard iPro system. The wetting characteristic of the coated and uncoated substrates was determined by measuring the water contact angle (WCA) using a drop shape analysis system (DSA-100, Krüss GmbH). Five measurements at different points of each sample were taken, and the average and standard deviation reported. Scanning Electron Microscopy (SEM) images were obtained using a FEI-SEM, FEI Inspect F. ImageJ software[38] was used to obtain the particle size distribution through SEM image analysis.

Results and discussion
Morphological, optical, and electrical properties

The Cu UTMF annealing was performed at low temperature (390 °C), i.e., sufficiently close to the temperature at above which dewetting of the continuous film is observed and below the glass strain point of the substrate (580 °C). By doing so, we intentionally introduce a degree of inhomogeneity into the contact angle, size and morphology of the particles obtained such that the plasmonic resonance effect on the coloring of the coating is kept within acceptable values. To provide a comparison and demonstrate the advantage of low temperature dewetting, a theoretical and experimental study was performed to compare high temperature (750 °C) and low temperature (390 °C) annealing cases. The study was performed on fused silica substrates because they have a higher strain point temperature (893 °C) and can withstand the 750 °C annealing condition without deformation. Electromagnetic simulations were performed using Finite Element Method with commercial COMSOL Multiphysics® software[39]. The theoretical model, detailed in the Supplementary Note 1, is based on a simplified 2D array of Cu

nanoparticles on glass substrate, and thus enables a qualitative rather than quantitative comparison with experimental data, still reproducing the experimental trends. The unit cells used for the simulations for the two different geometries are provided in Supplementary Fig. 3. Experimentally we observed that: (i) low temperature produces flatter nanoparticles with a lower contact angle, (ii) nanoparticles are much closer together, and in some cases, in contact with each other (Fig. 2a), (iii) high temperature annealing produced the typical narrowband resonance centered around 580 nm with pinkish color, while the same process at low temperature produced a broader resonance at longer wavelength with paler bluish color (Fig. 2b). The mean dewetted particle size was 72 nm ± 24 nm and 55 nm ± 16 nm for the low and high temperature dewetting cases, respectively. Note that in the case where the particle is non-spherical, the particle size refers to the longest lateral edge to edge distance of the feature. The simulated optical spectra show a trend in good agreement with the experimental observations and support a red-shift and broadening of the plasmonic resonance in the low temperature annealing condition due to a lower contact angle, this being consistent with previous work[33]. The change in particles' structure and associated optical response give the coating a transparency without strong dependence on wavelength. We have also measured low scattering (haze) <1%. The inset of Fig. 2b shows transparency and color neutrality of the low temperature dewetted TANCS against white and colored text backgrounds. The TANCS remains visually close to the neutral color of the substrate and have a transmission between 70–80% that is almost independent of wavelength in the visible range. Product modeling for capacitive touch devices was also performed for the TANCS using the Finite Element Model (Supplementary Fig. 2). The predictions show that our TANCS coatings do not prohibitively impact the scale and frequency dependence of the surface-lateral electrical impedance in the 1 MHz to 100 MHz frequency range required by touch-enabled devices. This suggests that TANCS coatings on glass would retain touch screen functionality.

AM activity of TANCS

Mock and AM testing was performed on TANCSs, whose conditions are presented in Table 1. A practical requirement for touch screen application is the ability to continually release Cu ions in optimal concentrations over a long period of time without compromising the overall transparency, durability, and functionality of the coating. Figure 3a plots the data of LR from AM test against the data of Cu leaching from the mock test. Raw data for the AM testing is provided in Supplementary Table 1. The LR correlates positively with the amount Cu leached into the solution up to ~4 mg/L after which increased Cu dissolution does not significantly increase the LR. By this, we determined the minimum inhibitory concentration of Cu (MIC-Cu) needed in solution to reach the EPA requirement of 3-LR, equivalent to 99.9% kill, to be ~2 mg/L. The bacterial killing mechanism could be explained by diffusion of mobile Cu ions through the SiO$_2$ and fluorosilane capping layers to the coating's surface where they interact with and kill the suspended/floating microbes. The diffusion of Cu ions is mediated by a liquid vehicle - e.g., cleaning solvents, surface moisture or the PBS solution hosting the bacteria. Based on a MIC-Cu of ~2 mg/L and, assuming a uniform distribution of microorganisms in the fluid, the number of ions, n, available to each microorganism are in the order of 10^{11} (see calculations provided in Supplementary Table 2 and Supplementary Fig. 4). This is orders of magnitude over the natural intracellular concentration of Cu atoms/ions in *S.Aureus*, which is reported to be in the region of 10^4–10^5 [40]. Therefore, it is reasonable to assume that TANCSs impose their AM activity by releasing Cu ions in sufficient concentrations for this specific bacteria. In general, the AM action due to the release of the ions is due to a combination of the material and the surface geometry. The presence of nanoparticles enhances the release of the ions compared to the bulk as the surface/volume ratio is higher[41].

For assessment of the optical properties, the transmission of the coatings in the visible region was measured before and after mock testing. Figure 3b shows the optical spectra and photographs corresponding to TANCS leaching <2 mg/L Cu (squares) and >4 mg/L Cu (circles). Both

cases show an increase in transmission after mock testing in the region of the plasmonic resonance associated with the Cu DNPs. This can be explained by reduced plasmonic coupling, as Cu dissolves into solution, the DNPs decrease in dimensions, reducing the interactions that give rise to plasmonic coupling. The distinction between Set A and B lies in the strength and duration of oxygen plasma cleaning treatment prior to the fluorosilane application. Set A TANCSs were treated with 50 W for 2 min whilst Set B were treated with 300 W for 5 min (see Table 1). The inset photographs in (b) show prototypical examples of TANCSs from both Sets after mock testing where the marked central region denotes the mock testing area. A distinction in the color of the central region after mock testing is observed where Set B maintains a color close to the original coating whilst Set A has a more evident color loss. The release of Cu species into the PBS droplet is influenced by the Cu solubility within the coating. It is likely that the different oxygen plasma treatment supports the difference in the leaching data between Set A and B TANCSs.

Optimizing the release of Cu with SiO$_2$ and fluorosilane capping layers

It is evident from the plot in Fig. 3a that some of the TANCSs in Table 1 leach Cu excessively above the MIC-Cu determined to be ~ 2 mg/L. From a coating longevity point of view, excessive Cu leaching is undesirable. In cases where [Cu] leached >> MIC-Cu, we propose that the Cu is being released in a burst like manor. The migration of chloride ions into the TANCS facilitates the fast generation of Cu ions such that the effect of the SiO$_2$ thickness is masked. To combat this and increase the longevity of the TANCS, we increased both the fluorosilane concentration and the SiO$_2$ thickness in order to control the rate of Cu dissolution.

The results are presented in Fig. 4 which plots the LR from the AM test and [Cu] leached during the mock test vs. SiO$_2$ thickness and fluorosilane concentration for TANCS treated with (a) 50 W and (b) 300 W oxygen plasma. First, we observe that Set A TANCSs leached up to four times more Cu than Set B for the same SiO$_2$ thickness and flurosilane concentration.
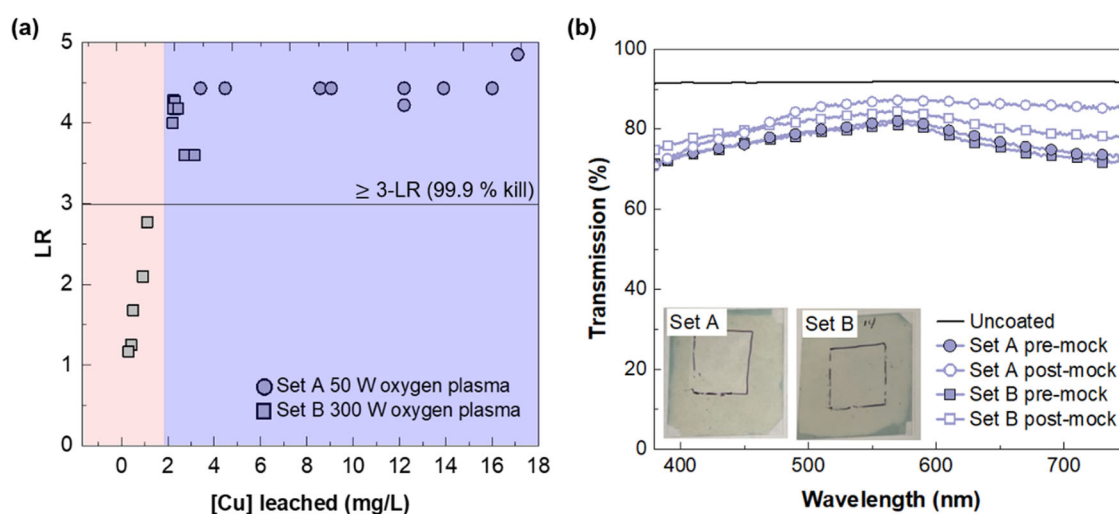

Fig. 3 | Antimicrobial properties of TANCS. a LR vs [Cu] leached. The EPA-prescribed 3-LR, corresponding to >99.9% reduction in bacterial colony counts, is marked with a black line. The blue and pink shaded regions correspond to the [Cu] range above and below which a 3-LR was observed, respectively. *The comparison between LR and [Cu] leached assumes that the majority of the ions are held in the liquid phase and not consumed by the microorganisms i.e., rate of Cu dissolution due to the PBS >> rate of consumption of Cu due to the presence of microorganisms. **b** Transmission spectra of representative TANCSs. For both graphs, the circle and square markers represent TANCSs from Sets A and B, respectively. Inset of (**b**) shows photographs of Set A and Set B after mock testing where the marked central region marked shows the testing area of 1×1 in.^{2}.
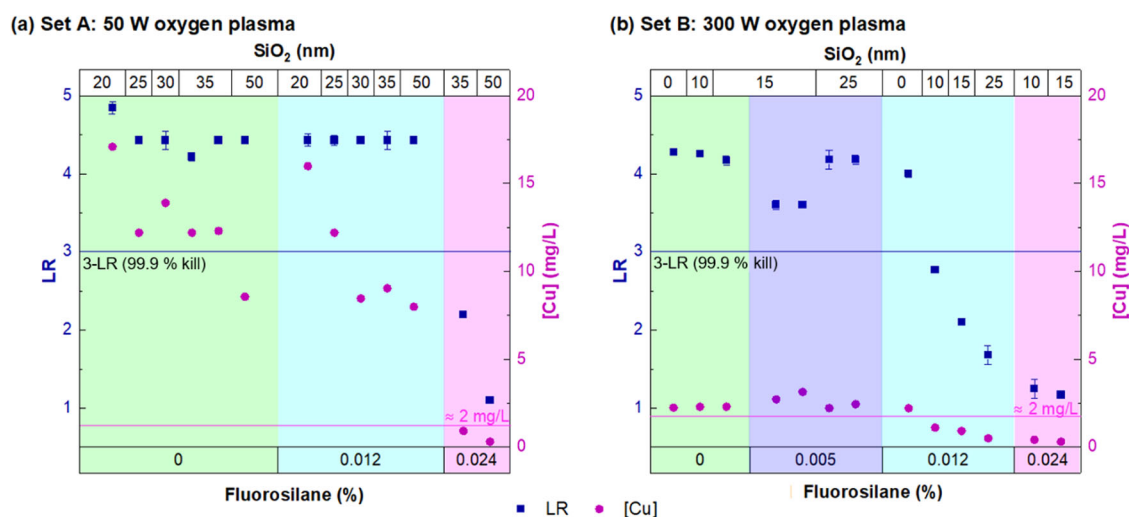

Fig. 4 | Plots of LR and [Cu] leached as a function of SiO$_2$ thickness and fluorosilane concentration. TANCSs were treated with 50 W and 300 W oxygen plasma in (**a**) and (**b**) respectively. Error bars represent the standard deviation of two samples. Note that in some cases, the error bar is smaller than the marker and not visible.
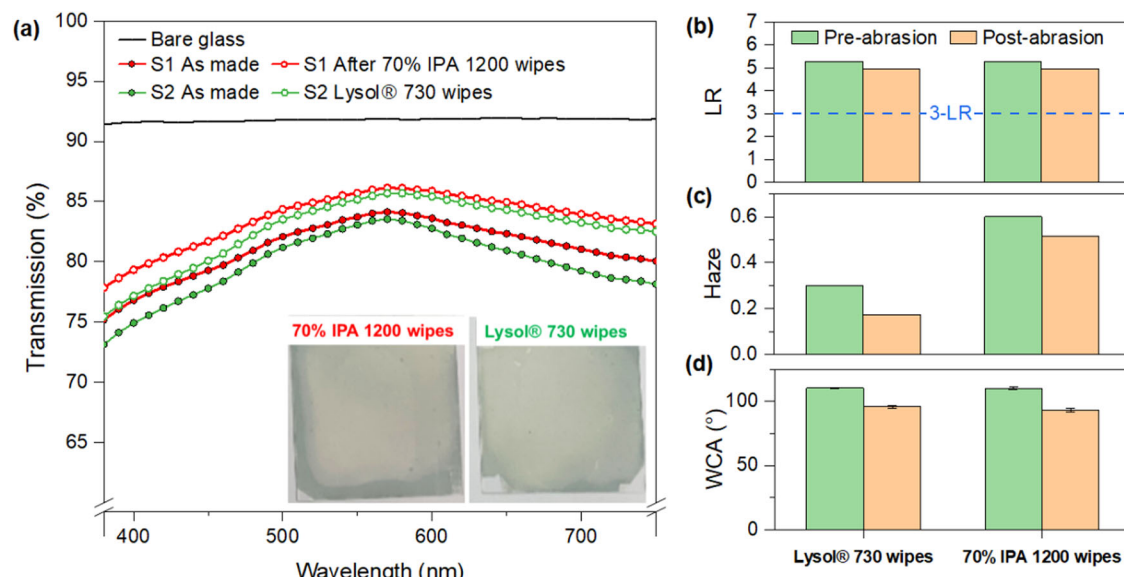
Fig. 5 | Optical and abrasion-resistance properties of TANCSs. a Transmission, **b** LR, **c** Haze, and **d** WCA of TANCSs before and after wet abrasion testing with IPA (1200 wipes) and Lysol® (730 wipes). The inset of (**a**) shows the TANCSs after wet abrasion testing on the central region. The size of the samples is 2×2 in.² The visual appearance of the central wiping region remains close in color to the outer region, indicting a good durability of the coating to repeated wipes with cleaning sanitizers.

The lower Cu dissolution rate in Set B is likely due to a higher (300 W) oxygen plasma treatment that may have partially oxidized the underlying Cu, thereby reducing its solubility. Second, we note that all TANCSs from Set A demonstrated a >4-LR in the AM test irrespective of SiO_2 thickness, except with the 0.024 % fluorosilane coated TANCSs, where the LR and [Cu] leached scaled inversely with SiO_2 thickness. The same trend was observed in Set B TANCSs, though, the effect of SiO_2 thickness was also observed for the lower (0.012%) fluorosilane concentration. It is likely that for TANCSs with high concentration fluorosilane high oxygen plasma treatment (Set B), the migration of chloride into the TANCS is reduced and the burst release mechanism is suppressed. In such a way, we demonstrate a method of controlling the Cu dissolution to within the optimal range above MIC-Cu. Overall, a combination of SiO_2 thickness, fluorosilane concentration and oxidation of the underlying Cu is required to achieve the optimal Cu release and LR.

Finally, the WCA of the coatings before and after AM testing was measured. The ETC coating imparts a contact angle >90° and changes by less than 5% after the AM test. Supplementary Table 3 shows that for the selected embodiments, after AM testing, the change in water contact angle of the AM-tested surfaces varies by less than 5% from the initial contact angle value of the coating measured before testing. For other samples, the variation is as low as 3% or less than 1%. The results of the AM testing illustrate good performance of the AM surface in terms of retaining a high water contact angle.

AM durability

Touchscreens are continuously exposed to various types of contact and wear. Therefore, durability and resistance to general wear and tear are important reliability features for AM coatings. Durability against wiping and cleaning, as prescribed by European Centre for Disease Prevention and Control (ECDC) guidelines for infection control, was tested by subjecting the TANCSs to up to 2 years of wear (see methods "Stipulated wear testing") and then testing their AM, optical and wetting properties. Identical TANCSs (each with 25 nm SiO_2 and 0.012% fluorosilane) were fabricated. One sample was immediately AM tested, and the second sample was AM tested after 730 or 1200 abrasion cycles with a Lysol® (sample S2) or IPA (sample S1) impregnated scouring pad on the coating surface, respectively. The results are presented in Fig. 5. The raw water contact angle data for samples S1 and S2 can be found in the Supplementary Table 4. All TANCSs demonstrated a >3-LR against *S. Aureus* even after abrasion testing. The TANCSs also maintained their wetting and optical characteristics post-abrasion, revealing a less than 5% average gain in transmission and between $10-15$% reduction in contact angle with respect to the initial value. The maintenance of the high WCA, demonstrates that the fluorosilane is robust topcoat that does not degrade with repeated wiping. Overall, the results of the abrasion test suggest that the embedded Cu DNPs are reasonably durable in terms of retaining AM activity, optical properties and high-WCA (>90°).

Conclusions

In this work, we have demonstrated the incorporation of Cu DNPs into a transparent and AM nanostructured Cu surface (TANCS) for glass substrates. The TANCS demonstrated a >99.9% reduction effectiveness against *S. Aureus* within 2 h, and have a color-neutral optical transmission, including the substrate, between 70–80% in the region 380–750 nm. Moreover, the TANCSs are easy to clean and retain their AM efficacy, optical, and wetting properties even after durability testing. In addition, they are fabricated in a way that is industrially scalable. We anticipate that the proposed TANCS may be useful in applications of technological interest such as multi-user transparent touch activated surfaces.

Data availability

Data generated during and/or analyzed during the current study are included in this published article (and its Supplementary Information file). Detailed reports that support the findings in this study are available from the corresponding author upon reasonable request.

References

1. Leyland, N. S. et al. Highly efficient F, Cu doped TiO2 anti-bacterial visible light active photocatalytic coatings to combat hospital-acquired infections. *Sci. Rep.* **6**, 24770 (2016).
2. Choi, H. J. et al. Enhanced transparency, mechanical durability, and antibacterial activity of zinc nanoparticles on glass substrate. *Sci. Rep.* **4**, 6271 (2014).

3. Dong, Y., Liu, T., Sun, S., Chang, X. & Guo, N. Preparation and characterization of SiO2/polydopamine/Ag nanocomposites with long-term antibacterial activity. *Ceram. Int.* **40**, 5605–5609 (2014).

4. Kastus Patent No. US20160312039A1.

5. Borrelli, N. F., Senaratne, W., Wei, Y. & Petzold, O. Physics and chemistry of antimicrobial behavior of ion-exchanged silver in glass. *ACS Appl. Mater. Interfaces* **7**, 2195–2201 (2015).

6. Schmidt, M. G. et al. Sustained reduction of microbial burden on common hospital surfaces through introduction of copper. *J. Clin. Microbiol.* **50**, 2217–2223 (2012).

7. Schmidt, M. G. et al. Copper surfaces are associated with significantly lower concentrations of bacteria on selected surfaces within a pediatric intensive care unit. *Am. J. Infect. Control* **44**, 203–209 (2016).

8. Gross, T. M. et al. Copper-containing glass ceramic with high antimicrobial efficacy. *Nat. Commun.* **10**, 1979 (2019).

9. Mitra, D., Li, M., Kang, E. T. & Neoh, K. G. Transparent copper-based antibacterial coatings with enhanced efficacy against pseudomonas aeruginosa. *ACS Appl. Mater. Interfaces* **11**, 73–83 (2019).

10. Behzadinasab, S. et al. Transparent and sprayable surface coatings that kill drug-resistant bacteria within minutes and inactivate SARS-CoV-2 Virus. *ACS Appl. Mater. Interfaces* **13**, 54706–54714 (2021). acsami.1c15505.

11. Kim, Y. H. et al. Preparation and characterization of the antibacterial Cu nanoparticle formed on the surface of SiO2 nanoparticles. *J. Phys. Chem. B* **110**, 24923–24928 (2006).

12. Varghese, S. et al. Antimicrobial activity of novel nanostructured Cu-SiO2 coatings prepared by chemical vapour deposition against hospital related pathogens. *AMB Express* **3**, 53 (2013).

13. Mitra, D., Kang, E. T. & Neoh, K. G. Antimicrobial copper-based materials and coatings: potential multifaceted biomedical applications. *ACS Appl. Mater. Interfaces* **12**, 21159–21182 (2020).

14. Mitra, D., Li, M., Kang, E. T. & Neoh, K. G. Transparent copper-loaded chitosan/silica antibacterial coatings with long-term efficacy. *ACS Appl. Mater. Interfaces* **9**, 29515–29525 (2017).

15. Raghunath, A. & Perumal, E. Metal oxide nanoparticles as antimicrobial agents: a promise for the future. *Int. J. Antimicrob. Agents* **49**, 137–152 (2017).

16. Scully, R. J. The COVID-19 pandemic, Part 1: can antimicrobial copper-based alloys help suppress infectious transmission of viruses originating from human Contact with high-touch surfaces? *Corrosion* **76**, 524–527 (2020).

17. Nakhaie, D. et al. An engineered nanocomposite copper coating with enhanced antibacterial efficacy. *Adv. Mater. Interfaces* **9**, 2201009 (2022).

18. Bogdanović, U. et al. Nanomaterial with high antimicrobial efficacycopper/polyaniline nanocomposite. *ACS Appl. Mater. Interfaces* **7**, 1955–1966 (2015).

19. Lex, J. R. et al. Megaprosthesis anti-bacterial coatings: a comprehensive translational review. *Acta Biomater.* **140**, 136–148 (2022).

20. Ning, C. et al. Concentration ranges of antibacterial cations for showing the highest antibacterial efficacy but the least cytotoxicity against mammalian cells: implications for a new antibacterial mechanism. *Chem. Res. Toxicol.* **28**, 1815–1822 (2015).

21. Valko, M., Morris, H. & Cronin, M. T. D. Metals, toxicity and oxidative stress. *Curr. Med. Chem.* **12**, 1161–1208 (2005).

22. Angelé-Martínez, C., Nguyen, K. V. T., Ameer, F. S., Anker, J. N. & Brumaghim, J. L. Reactive oxygen species generation by copper(II) oxide nanoparticles determined by DNA damage assays and EPR spectroscopy. *Nanotoxicology* **11**, 278–288 (2017).

23. Yoon, K. Y., Hoon Byeon, J., Park, J. H. & Hwang, J. Susceptibility constants of Escherichia coli and Bacillus subtilis to silver and copper nanoparticles. *Sci. Total Environ.* **373**, 572–575 (2007).

24. Chatterjee, A. K., Chakraborty, R. & Basu, T. Mechanism of antibacterial activity of copper nanoparticles. *Nanotechnology* **25**, 135101 (2014).

25. Vincent, M., Hartemann, P. & Engels-Deutsch, M. Antimicrobial applications of copper. *Int. J. Hyg. Environ. Health* **219**, 585–591 (2016).

26. Mahmoodi, S., Elmi, A. & Hallaj Nezhadi, S. Copper nanoparticles as antibacterial agents. *J. Mol. Pharm. Org. Process Res.* **06**, 1–7 (2018).

27. Grass, G., Rensing, C. & Solioz, M. Metallic copper as an antimicrobial surface. *Appl. Environ. Microbiol.* **77**, 1541–1547 (2011).

28. Vincent, M., Duval, R. E., Hartemann, P. & Engels-Deutsch, M. Contact killing and antimicrobial properties of copper. *J. Appl. Microbiol.* **124**, 1032–1046 (2018).

29. Wang, S. et al. Antibacterial nanostructured copper coatings deposited on tantalum by magnetron sputtering. *Mater. Technol.* **30**, B120–B125 (2015).

30. Bharadishettar, N., Bhat K, U. & Panemangalore, D. B. Coating technologies for copper based antimicrobial active surfaces: a perspective review. *Metals* **11**, 711 (2021).

31. Hosseini, M. et al. Transparent anti-SARS-CoV-2 and antibacterial silver oxide coatings. *ACS Appl. Mater. Interfaces* **14**, 8718–8727 (2022).

32. United States Environmental Protection Agency. *Test Method for Efficacy of Copper Alloy Surfaces as a Sanitizer* (United States Environmental Protection Agency, Washington DC, 2015).

33. Yu, R. et al. Structural coloring of glass using dewetted nanoparticles and ultrathin films of metals. *ACS Photonics* **3**, 1194–1201 (2016).

34. Rombaut, J., Fernandez, M., Mazumder, P. & Pruneri, V. Nanostructured hybrid-material transparent surface with antireflection properties and a facile fabrication process. *ACS Omega* **4**, 19840–19846 (2019).

35. Mazumder, P. et al. Superomniphobic, transparent, and antireflection surfaces based on hierarchical nanostructures. *Nano Lett.* **14**, 4681 (2014).

36. Thompson, C. V. Solid-state dewetting of thin films. *Annu. Rev. Mater. Res.* **42**, 399–434 (2012).

37. Leroy, F. et al. How to control solid state dewetting: a short review. *Surf. Sci. Rep.* **71**, 391–409 (2016).

38. Schindelin, J. et al. Fiji: an open-source platform for biological-image analysis. *Nat. Methods* **9**, 676–682 (2012).

39. COMSOL AB, S. S. COMSOL Multiphysics® software. v.6.1. www.comsol.com.

40. Finney, L. A. & O'halloran, T. V. Transition metal speciation in the cell: insights from the chemistry of metal ion receptors. *J. Appl. Crystallogr.* **277**, 869 (2002).

41. Karlsson, H. L. et al. Cell membrane damage and protein interaction induced by copper containing nanoparticles-Importance of the metal release process. *Toxicology* **313**, 59–69 (2013).

Acknowledgements

Author contributions

The manuscript was written through contributions of all authors. All authors have given approval to the final version of the manuscript. Valerio Pruneri and Wageesha Senaratne designed research; Christina Graham performed the fabrication experiments and data analysis, wrote the manuscript and prepared all figures; Alessia Mezzadrelli performed the COMSOL modeling and contributed to the writing; Prantik Mazumder helped with the

Competing interests

C.G., W.S., D.T., and V.P. are co-inventors of a patent application (US Provisional Patent Application No. 63/609,463) related to the results of this paper. All other authors declare no competing interests.

Additional information

Supplementary information The online version contains supplementary material available at https://doi.org/10.1038/s43246-024-00472-w.

Correspondence and requests for materials should be addressed to Wageesha Senaratne or Valerio Pruneri.

Reprints and permissions information is available at http://www.nature.com/reprints

Publisher's note Springer Nature remains neutral with regard to jurisdictional claims in published maps and institutional affiliations.